Chin. J. Astron. Astrophys. Vol. 6 (2006), No. 1, 96–112
(*http://www.chjaa.org*)

Chinese Journal of
Astronomy and
Astrophysics

Magnetic Helicity Injection in Solar Active Regions *

Hong-Qi Zhang

National Astronomical Observatories, Chinese Academy of Sciences, Beijing 100012;
hzhang@bao.ac.cn

Received 2005 May 21; accepted 2005 October 27

Abstract We present the evolution of magnetic field and its relationship with magnetic (current) helicity in solar active regions from a series of photospheric vector magnetograms obtained by Huairou Solar Observing Station, longitudinal magnetograms by MDI of SOHO and white light images of TRACE. The photospheric current helicity density is a quantity reflecting the local twisted magnetic field and is related to the remaining magnetic helicity in the photosphere, even if the mean current helicity density brings the general chiral property in a layer of solar active regions. As new magnetic flux emerges in active regions, changes of photospheric current helicity density with the injection of magnetic helicity into the corona from the subatmosphere can be detected, including changes in sign caused by the injection of magnetic helicity of opposite sign. Because the injection rate of magnetic helicity and photospheric current helicity density have different means in the solar atmosphere, the injected magnetic helicity is probably not proportional to the current helicity density remaining in the photosphere. The evidence is that rotation of sunspots does not synchronize exactly with the twist of photospheric transverse magnetic field in some active regions (such as, delta active regions). They represent different aspects of magnetic chirality. A combined analysis of the observational magnetic helicity parameters actually provides a relative complete picture of magnetic helicity and its transfer in the solar atmosphere.

Key words: Sun: activity – Sun: magnetic fields

1 INTRODUCTION

It is generally believed that the magnetic energy transfer from the subatmosphere into the corona is reflected in the evolution of the photospheric vector magnetogram, even if the configuration of magnetic field has been distorted by surface processes such as advection and diffusion during the emergence of the active region. By following it, one probably can construct a basic model of the formation of magnetic field and its relationship with solar activities.

The magnetic and current helicities provide some information on the handedness and also non-potentiality of the magnetic field in the solar atmosphere. As a twisted magnetic field emerges from the subatmosphere, it provides important information on the generation of twisted magnetic field in the subatmosphere and on the injection of magnetic helicity in the solar atmosphere. Magnetic helicity is a quantitative measure of global chiral properties of the magnetic field in the solar atmosphere and it can change either because of emergence of some new twisted field across the photospheric surface or by horizontal motion on the latter. The relationship between the motion of magnetic footpoints in the photosphere and helicity injection has been discussed by some authors (Chae 2001; Nindos & Zhang 2002).

* Supported by the National Natural Science Foundation of China.

Magnetic helicity is not immediately observable, in contrast with the current helicity density in the solar photosphere. The current helicity is also an important index for analyzing the chirality of the magnetic field. Vector magnetogram observations provide an opportunity to diagnostic the existence of current helicity density. The evolution of current helicity density in active regions in the photosphere were analyzed by Pevtsov et al. (1994) and Zhang (2001a). A relationship between change in photospheric current helicity density and solar flares was found by Bao et al. (1999). A notable evidence is the sign rule of helicity: most active regions show negative (positive) mean current helicity density in the northern (southern) hemisphere (Seehafer 1990). It provides some correlation between the magnetic field and helicity from the subatmosphere (Longcope et al. 1998; Kleeorin et al. 2003).

In this paper, we study the formation of magnetic (current) helicity in the solar atmosphere. We consider the evolution of the magnetic field and the relationship with magnetic (current) helicity in the relative simple active region NOAA 9033 and the delta active region NOAA 9077. We present the relationship between the injection of magnetic helicity from the subatmosphere and the evolution of photospheric current helicity density in the emerging flux region. We also demonstrate how the formation of non-potential magnetic field with its shear motion in the photosphere brings the magnetic (current) helicity into the higher atmosphere of the delta active region.

2 TWISTED MAGNETIC FIELD AND HELICITY

Magnetic helicity is defined as

$$H_m = \int_V h_m d^3x = \int_V \boldsymbol{A} \cdot \boldsymbol{B} d^3x, \tag{1}$$

where the vector potential $\boldsymbol{A}$ can not be observed immediately. Magnetic helicity is conserved in a closed volume where a small resistivity is present. Change of magnetic helicity in the solar atmosphere is related to motion of the footpoints of magnetic field at the solar surface (Berger & Field 1984)

$$\frac{dH_m}{dt} = -2 \oint_S [(\boldsymbol{V}_t \cdot \boldsymbol{A}_p) B_n - (\boldsymbol{A}_p \cdot \boldsymbol{B}_t) V_n] ds, \tag{2}$$

where the magnetic field $\boldsymbol{B}$ and velocity field $\boldsymbol{V}$ are observable quantities. The first term in Eq. (2) provides the contribution from a twisted motion of the footpoints, while the second term, from an emergence of twisted magnetic flux from the subatmosphere.

Figure 1 shows the two cases: Case 1 presents a possible configuration of magnetic flux and its relationship with mass motion in the vicinity of the footpoints of flux tubes in the photosphere. As the direction of motion is perpendicular to the direction of the magnetic field, due to the frozen-in effect, the mass motion provides information on that the magnetic field. The mass motion in the vicinity of the magnetic footpoints can in general be separated into an orthogonal and a parallel motion relative to the lines of force. The tangential component of the velocity field near the footpoints in the solar surface can be normally detected by the evolution of the photospheric (magnetic) features by means of the local correlation tracking technique. The relative twist of magnetic flux tubes can be confirmed by the collective motion of the corresponding magnetic features, the footpoints of magnetic lines of force in the solar surface.

Case 2 in Figure 1 presents another possibility on the emergence of twisted magnetic field: emergence of highly twisted magnetic flux tubes from the subatmosphere. This makes a similar contribution to the helicity injection to Case 1. Case 2, represented by the second term in right side of Eq. (2), was discussed by Kusano et al. (2002). An important improvement with a relative simple form was made by Demoulin & Berger (2003), where the horizontal motions, deduced by tracking the photospheric cut of magnetic flux tubes, include the effects of both the emergence and the shearing cases, however complex the magnetic configuration is. They also analyzed the observational difficulties involved in deriving the flux tubes. They derived

$$\frac{dH_m}{dt} = -2 \oint_S (\boldsymbol{U} \cdot \boldsymbol{A}_p) B_n ds, \tag{3}$$

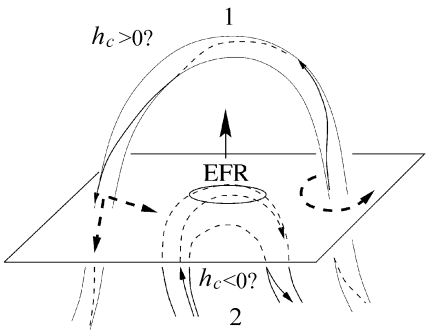

Fig. 1 Two basic possible models of the injection of magnetic helicity into the solar atmosphere. (1) Rotation of the footpoints of magnetic lines. The thick dash arrows mark possible motions of the mass, relative to the magnetic lines of force. (2) Twisted magnetic flux emerging from the subatmosphere.

where

$$\boldsymbol{U} = \boldsymbol{V}_t - \frac{V_n}{B_n}\boldsymbol{B}_t. \tag{4}$$

As a linked or twisted magnetic flux bundle emerges from the subatmosphere, its footpoints show sheared or twisted motion which can be analyzed by the equivalent form in Eqs. (3) and (4). This implies that one can not exclude the contribution of emerging flux in the horizontal motion of magnetic footpoints in the solar surface. In the following the injection of magnetic helicity from the motion of magnetic footpoints in the photosphere will be discussed.

The footpoint motion of magnetic field due to velocity vortex relates to the heterogeneity and twist of velocity field shown in the rotation of the magnetic field. It is similar to the analysis of the current (Zhang 2001b). Moreover, a problem is the uncertainties on the derived velocity vector from photospheric magnetic features (and also the corresponding morphological features) as these have been used to infer the rate of change of magnetic helicity. These relate to the spatial resolution and the undetectable motions of magnetic field, such as the proper motions of strong magnetic field inside sunspots that are normally undetectable in the magnetograms. Even though the velocity derived from the application of the local correlation tracking technique on the white light images probably provides higher spatial accuracy than that of magnetograms, accurate rate of change of the magnetic helicity in Eq. (3) inferred from the observational horizontal motions is still a problem awaiting solution (Chae 2001; Nindos & Zhang 2002).

Similar to Eq. (2), the local rate of change of magnetic helicity density can be written as (Berger & Field 1984)

$$\frac{dh_m}{dt} = -2\nabla \cdot [(\boldsymbol{V}_t \cdot \boldsymbol{A}_p)\boldsymbol{B} - (\boldsymbol{A}_p \cdot \boldsymbol{B}_t)\boldsymbol{V}]. \tag{5}$$

It means that the change of magnetic helicity density can be detected in principle from the local change of moving magnetic field. Because the quantitative measurement of moving magnetic field in a close surface in the solar atmosphere is difficult, the local injected rate of magnetic helicity density can not be obtained completely. On the other hand, as the highly sheared or twisted magnetic flux emerges from the solar subatmosphere, one probably can approximately obtain the basic observational information on the local injection of magnetic helicity density and find its relationship with the observed current helicity density in the solar surface (Zhang 2001a). This means that the local rate of change of magnetic helicity density from Eq. (3) can be written in the form,

$$\frac{dh_m}{dt} = f(G), \quad \text{where} \quad G = -2(\boldsymbol{U} \cdot \boldsymbol{A}_p)B_n, \tag{6}$$

even if the locally injected helicity does not remain in the lower atmosphere completely, because a part of magnetic helicity density is probably transferred along the magnetic lines of force into the

corona and interplanetary space (Berger & Field 1984; Longcope & Welsch 2000). For a bundle of flux tubes with uniformly distributed magnetic helicity density, the rate of change of magnetic helicity density from local motion of the footpoints in the solar surface can be estimated approximately as

$$\frac{dh_m}{dt} = \frac{G}{l}, \tag{7}$$

where l is the equivalent length of the flux tube. This means that, rotation of the footpoints of magnetic flux (or emergence of twisted magnetic flux) causes twist in the magnetic field above the photosphere, and a part of the twisted field probably remains in the lower layer of the solar atmosphere as the helicity is not completely ejected from the lower atmosphere. Figure 1 shows the two typical cases of injection of magnetic helicity with twist or emergence of magnetic flux. In the approximation of force free field, the relationship between the rate of change of magnetic helicity from the subatmosphere and the distribution of current helicity density in the photosphere becomes relative simple, with both showing the same signs (Wang 1996).

It is found that, unlike the magnetic helicity density, only a part (the vertical component) of the current helicity density in the photosphere can be inferred from the photospheric vector magnetograms, due to the observational limitation (Abramenko et al. 1996; Bao & Zhang 1998)

$$h_{cz} = \boldsymbol{B} \cdot (\nabla \times \boldsymbol{B})_z \,. \tag{8}$$

A similar limitation applies to the analysis by the force free factor (Pevtsov et al. 1994)

$$\alpha = \frac{\mu J_z}{B_z}, \tag{9}$$

which also does not contain any information on the horizontal component of the current helicity density. Even if the study on the evolution of current helicity density (or force free factor) in solar active regions provides some important information on the transfer of helicity from solar subatmosphere, the limited (and/or interrupted) observations of photospheric vector magnetograms can not give the temporal rate of change of current helicity density in the photosphere, similar to the magnetic helicity. The mean photospheric current helicity density (or mean force free factor) is normally used to infer the handedness of magnetic field in active regions for it has been found that the magnetic field probably twists with the same handedness in the high solar atmosphere: hence their importance in the analysis of global twist of magnetic field in active regions (Seehafer 1990; Pevtsov et al. 1995; Abramenko et al. 1996; Bao & Zhang 1998).

The 180°-ambiguity of transverse magnetic field comes from intrinsic properties of polarized light of lines in the measurements of magnetic field. It can only be resolved under some additional assumptions. It is normally believed that the transverse field points from positive to negative polarity in the solar surface, as the field is approximately potential there. Alternatively, continuity of the transverse field can be appealed to. The 180°-ambiguity of transverse components near a highly sheared magnetic neutral line in the photospheric vector magnetograms probably causes a loss of accuracy in the calculation of photospheric current helicity density in active regions, when the direction of the transverse field can not be decided on the basis of magnetic charge or potential field or continuity. It is noticed that the current helicity density inferred from local areas of highly sheared magnetic field is not dominant in the total contribution of current helicity. Even if such problems are present, difference in the distribution of the photospheric current helicity density h_{cz} inferred from vector magnetograms of different times actually carries information on the rate of change of current helicity density, and can be used to analyze its relationship with the magnetic helicity.

3 OBSERVATIONS

This paper uses photospheric vector magnetograms observed at Huairou Solar Observing Station (Ai et al. 1982; Ai & Hu 1987; Zhang & Ai 1986). Two working lines are used by the Huairou Vector Magnetograph with a birefringent filter of 1/8 Å bandpass: one is FeIλ5324.19 Å for photospheric

vector magnetograms and Dopplergrams (Ai et al. 1982), and the other is H$\beta\lambda$4861.34 Å for chromospheric longitudinal magnetograms and Dopplergrams (Zhang & Ai 1986). Comparisons of the vector magnetograms with other vector magnetographs have been made by Wang et al. (1992), Bao et al. (2000) and Zhang et al. (2003).

After the resolution of the 180°-ambiguity of the transverse components, the current helicity density h_{cz} and the force free factor α can be inferred by the photospheric vector magnetograms,

$$h_{cz} = \Big(\frac{\partial B_y}{\partial x} - \frac{\partial B_x}{\partial y}\Big)B_z \quad \text{and} \quad \alpha = \Big(\frac{\partial B_y}{\partial x} - \frac{\partial B_x}{\partial y}\Big)/B_z\,. \tag{10}$$

In the calculation of the helicity parameters, the errors mainly come from the differences between neighboring pixels in the observed transverse field. After smoothing down noise fluctuations in the calculation, the distribution of large-scale current helicity parameters in the photosphere is obtained.

Some longitudinal magnetograms analyzed in this paper were observed by MDI of SOHO satellite. For studying the morphological configuration of active regions, some white light and EUV 171 Å images observed by TRACE satellite, and soft X-ray images by YOHKOH satellite, have also been used.

4 TRANSFER OF MAGNETIC HELICITY

4.1 Emergence of Magnetic Flux in Active Region NOAA 9033

Figure 2 shows the evolution of magnetic field with newly emerging magnetic flux in the northern active region NOAA 9033 in June 2000. The arrow in Figure 2 indicates the position of a newly emerging magnetic flux in the large-scale negative following polarity of the active region. We can find some new magnetic features of positive polarity formed and moved westward gradually. The mean force free factor $\overline{\alpha}$ of NOAA 9033 on 2000 June 13 is $1.52\times10^{-9}\mathrm{m}^{-1}$ and the $\alpha_{\rm best}$ is $-6.2\times10^{-9}\mathrm{m}^{-1}$ for $Bz > 300$ G and $1.6\times10^{-9}\mathrm{m}^{-1}$ for $Bz > 800$ G. This means that the average twist of magnetic field in the whole active region is not significant compared to other highly twisted magnetic fields of active regions (Bao & Zhang 1998; Longcope et al. 1998; Zhang & Bao 1999).

Figure 3 shows a series of photospheric vector magnetograms in the emerging flux region (EFR) and the corresponding current helicity density h_{cz} inferred from Eq. (7) in the active region NOAA 9033. We find that the magnetic pole 'A' of positive polarity moved westward and separated from the negative polarity 'B', due to the emergence of magnetic flux. The transverse magnetic field of 'A' twisted clockwise gradually. After the calculation of current helicity density h_{cz} with the photospheric vector magnetograms, we find the current helicity density h_{cz} of magnetic features 'A' and 'B' changed sign in the period between June 11 and 12. To confirm this change, a series of Huairou photospheric vector magnetograms and corresponding maps of current helicity density h_{cz} on June 11 are shown in Figure 4. We find fluctuation of h_{cz} near 'A' and 'B'. It is probably caused by local interaction of magnetic field during the latter's emergence. We also find that the distribution of h_{cz} near other magnetic structures is relative stable on June 11. Figure 5 shows the Hβ chromospheric features and the magnetic field near the magnetic poles 'A' and 'B' of opposite polarities, which reveals short dark arch filaments in Hβ connected the two poles along the direction of the photospheric transverse field. This means the magnetic poles 'A' and 'B' are a pair of footpoints of an emerging magnetic bundle. The evolution of magnetic features 'A' and 'B' and the relationship with the photospheric current helicity density h_{cz} are consistent with emerging magnetic flux bringing magnetic helicity into the solar surface (Zhang 2001a).

To find possible reason for the change and evolution of the current helicity at the magnetic poles in the active region, we show in Figure 6 the rate of change of magnetic helicity due to the photospheric motion by the local correlation tracking technique (Chae 2001; Nindos & Zhang 2002). It is found that negative magnetic helicity density was injected near the magnetic features 'A' and 'B' in the following polarity of the active region on June 11 and 12. It is consistent with the increase of negative current helicity h_{cz} near 'A' and 'B' in Figure 3. The sign of current helicity density in 'A' and 'B' changed from positive to negative in the initial phase of the emergence of new magnetic flux on June 11 and 12 in Figure 3. This provides a piece of evidence on the injection of

negative magnetic helicity from the subatmosphere in the active region and on the contribution to the increase of photospheric negative current helicity density from the emerging magnetic dipole.

Similar cases can be found near magnetic features 'C' and 'D' in Figures 3 and 6, where the photospheric current helicity density h_{cz} changed at 02:49 UT on June 11 and at 04:23 UT on June 12. The negative current helicity density structures 'C' and 'D' inferred by photospheric vector magnetogram at 02:49 UT on June 11 almost disappeared at 04:23 UT on June 12 in Figure 3. By following the injection rate of magnetic helicity in Figure 6, we can show where the injection of positive magnetic helicity can be found. The relevant relationship between the current helicity density and injection of magnetic helicity also can be found near the twisted magnetic features E and F of positive polarity on June 11 and 12 in Figure 3. The evolution of corresponding photospheric current helicity density is insignificant and where the rate of change of magnetic helicity is almost negligible in Figure 6, even though the magnetic feature E with its positive current helicity disappeared gradually on June 13 and 14 in the collision with negative magnetic polarity.

Figure 7 shows the time profile of the accumulated change of magnetic helicity inferred from a series of magnetograms in the active region NOAA 9033 and the local regions as shown in Figure 6 by Eq. (3) and the mean current helicity density h_{cz} in Figure 3 in the period July 10–14. The mean value of h_{cz} on June 11 was used in Figure 7 in view of its fluctuation. This fluctuation is mainly caused by the change of sign of the current helicity density in the magnetic feature 'A' on June 11. The mean values on June 12, 13 and 14 are average values inferred separately from the relevant vector magnetograms. It is revealed that an amount of negative magnetic helicity was injected from the subatmosphere in the active region, while the local rate of injection of magnetic helicity (related to the evolution of the magnetic features and the corresponding current helicity density) is not obvious, but it does not influence the identification on the injection of magnetic helicity related to the emergence of magnetic flux in the solar surface in Figure 6. The total injection rate of magnetic helicity in the local area in Figure 6 does not reflect the global properties of the whole active region. Moreover, the different evolutionary tendencies in Figure 7 between injection of negative magnetic helicity from the subatmosphere and change of mean current helicity density in the solar photosphere show that the evolution of photospheric current helicity density loses information on the accumulation of helicity above the photosphere, even though the photosphere is an important layer for detecting transfer of helicity from the subatmosphere.

4.2 Twisted Motion in Active Region NOAA 9077

4.2.1 Highly Sheared Magnetic Field Near Magnetic Neutral line

Figure 8 traces the formation of a highly sheared spatial configuration of the magnetic field in the active region inferred from a series of photospheric vector magnetograms of the delta active region NOAA 9077. It is shown that the photospheric main pole 'N1' of positive polarity moved westward at a speed of about 0.1–0.2 km s^{-1} and squeezed the negative magnetic pole 'S1'. The penumbral feature S1 disappeared gradually with the decrease and breakup of the sunspot umbra 'N1'. The photospheric transverse magnetic field between the opposite poles 'N1' and 'S1' was almost parallel to the magnetic neutral line on July 12 and 13, forming the magnetic shear. The shear of transverse field near the magnetic neutral line between the opposite magnetic poles 'N1' and 'S1' gradually decreased on June 14 and 15. In Figure 8, 'A' marks an eastward moving sunspot relative to the whole active region, which separated away from the sunspot umbra 'N1' significantly in the period of July 12–14. Figure 9 shows the relationship between the photospheric vector magnetic field, the TRACE and soft X-ray images in the active region on July 14. The intense soft X-ray emission occurred near the magnetic neutral line. By comparing the relationship between the photospheric transverse magnetic field and the 171 Å features near 'A', 'N1' and 'S2', their consistency can be found. The TRACE 171 Å features actually inform on the direction of magnetic field above the photosphere. Near the magnetic neutral line NL a difference in the orientation between the photospheric transverse magnetic field and the TRACE 171 Å features can be noted, where the TRACE features show highly sheared magnetic lines of force above the photosphere in different directions to the photospheric transverse field. The distribution of the large-scale soft

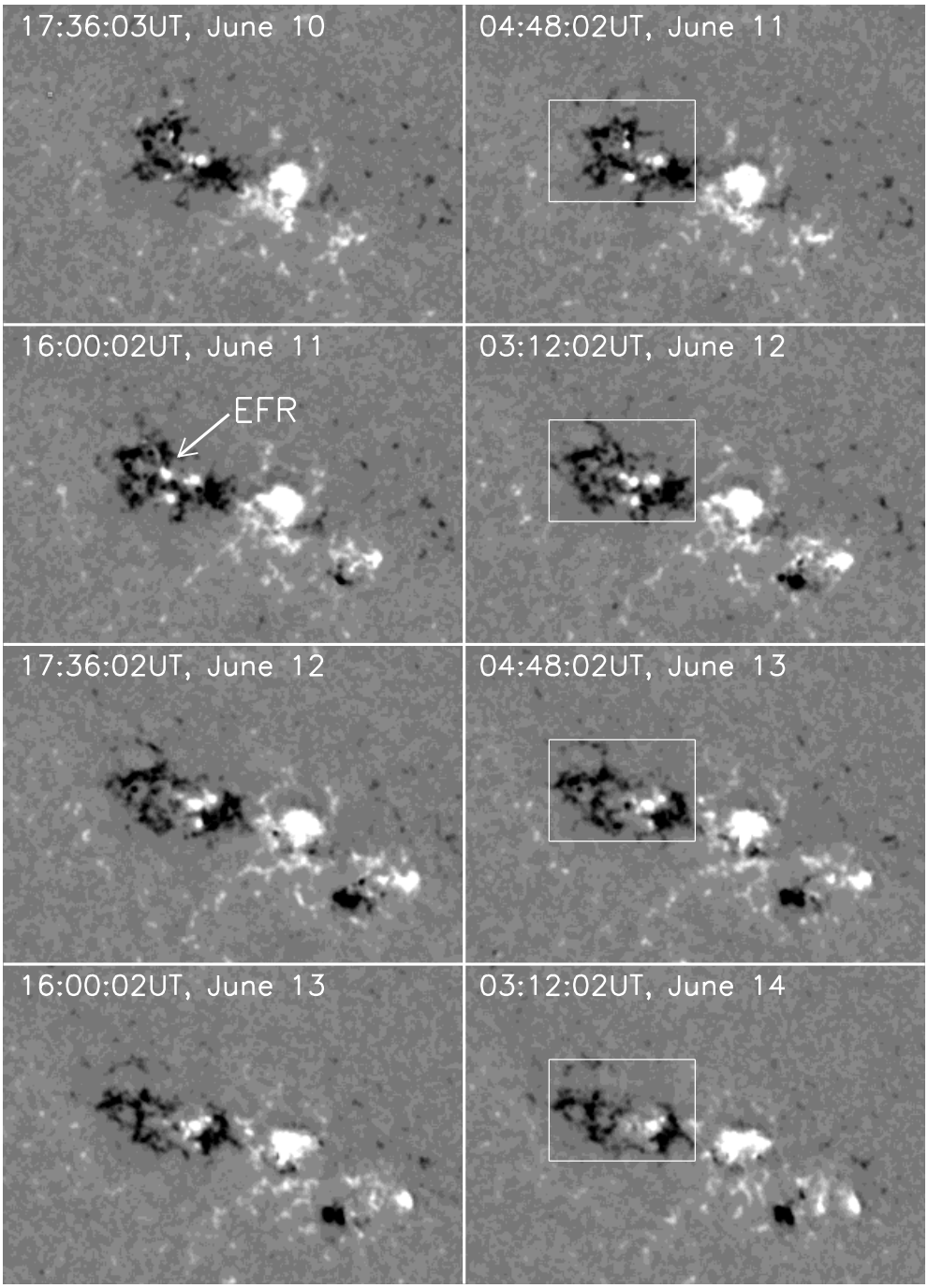

Fig. 2 Evolution of photospheric longitudinal magnetic field in active region NOAA 9033 in 2000 June. White (black) marks positive (negative) polarity. The rectangles mark the areas of the following magnetic structures. See the text and Figures 3 and 4. North on top and west to the right.

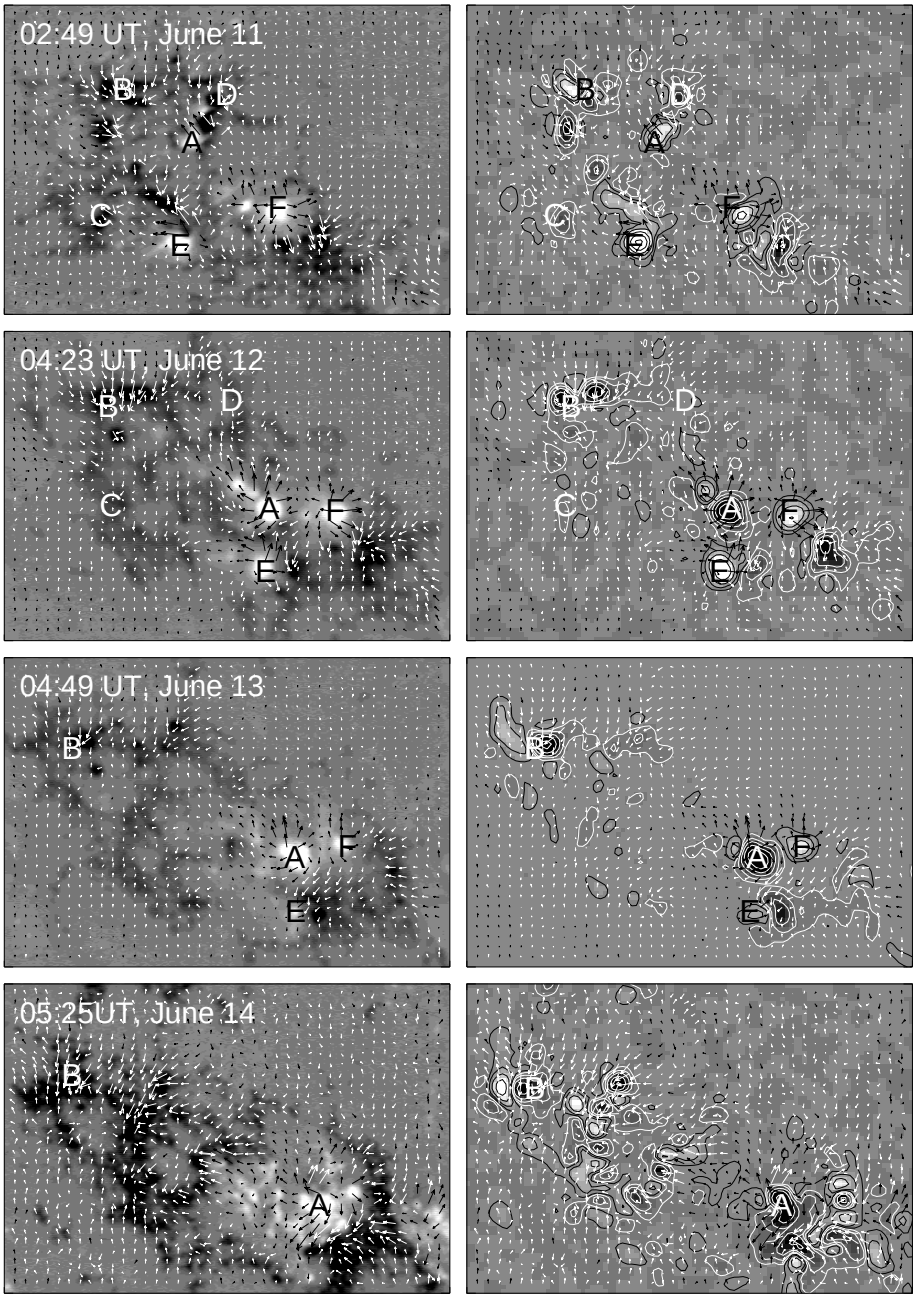

Fig. 3 Local photospheric vector magnetograms in active region NOAA 9033 in 2000 June (left). White (black) marks positive (negative) polarity. The corresponding map of photospheric current helicity density is shown (right), where white (black) marks positive (negative) density of h_{cz} of ± 5, 20, 100, 180, 300 ($\times 10^{-3}\mathrm{G}^2\mathrm{m}^{-1}$). The arrows indicate the transverse magnetic field. The size of the maps is $3.1' \times 2.1'$. The corresponding areas in Fig. 2 are marked by the rectangles.

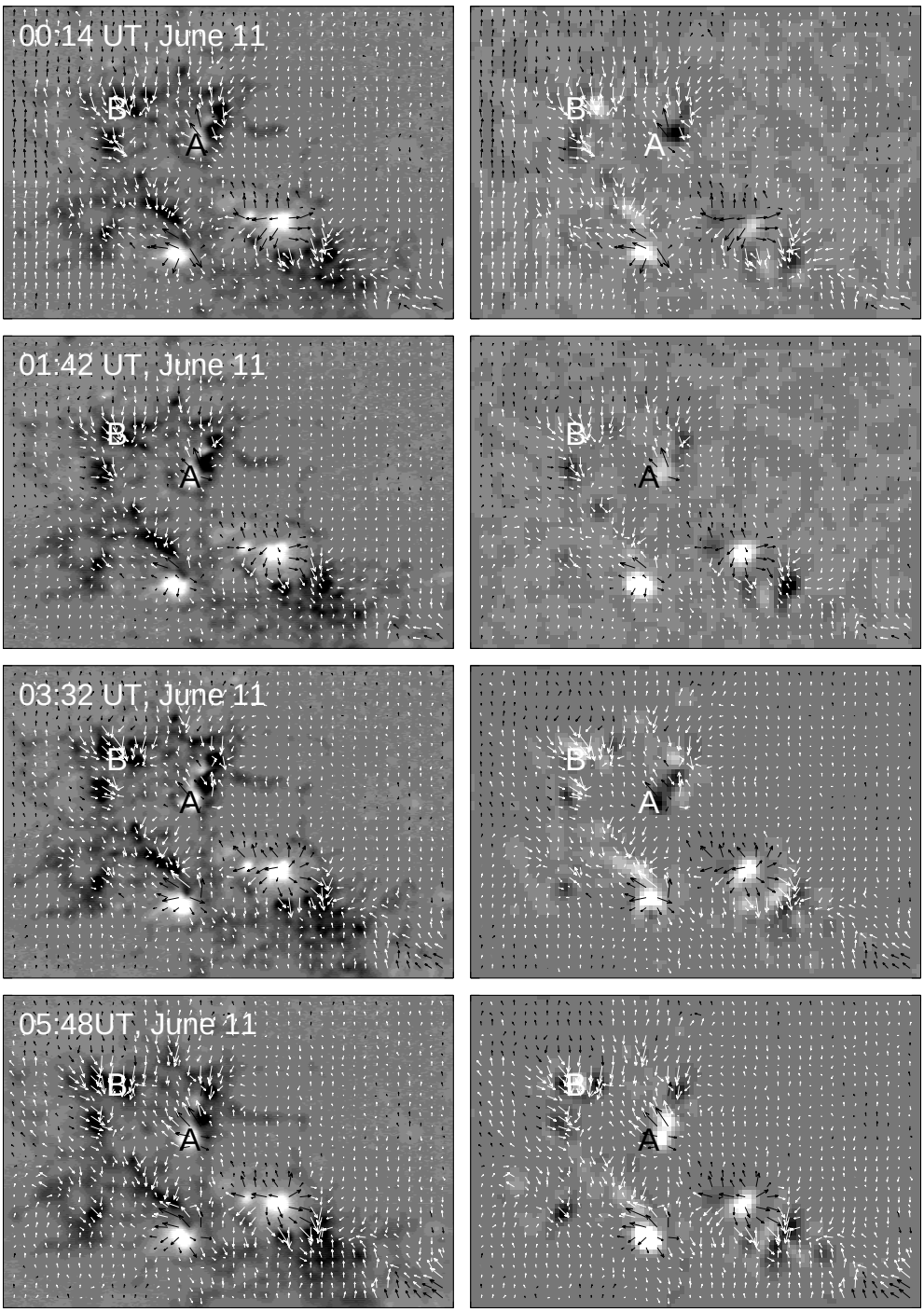

Fig. 4 Local photospheric vector magnetograms in active region NOAA 9033 on 2000 June 11 (left), where white (black) marks positive (negative) polarity. The corresponding photospheric current helicity density map is shown (right), where white (black) marks positive (negative) density. The arrows indicate the transverse magnetic field. The size of maps is $3.1' \times 2.1'$. The corresponding areas in Fig. 2 are marked by the rectangles.

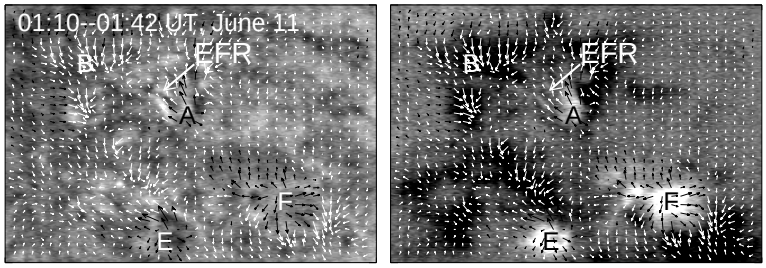

Fig. 5 Local Hβ chromospheric filtergram (left) and the corresponding longitudinal magnetogram (right) in active region NOAA 9033 at 01:10 UT on June 11, where white (black) marks positive (negative) polarity. The arrows indicate the photospheric transverse magnetic field observed at 01:42 UT.

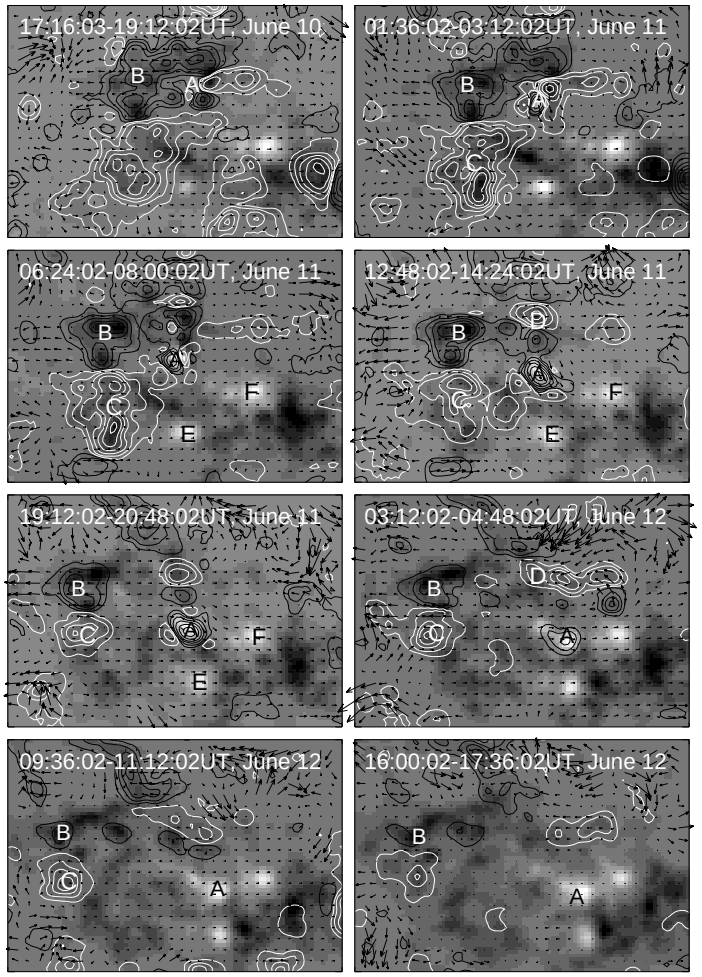

Fig. 6 Horizontal velocity vectors and the corresponding gray-scale maps of $G = -2\boldsymbol{U} \cdot \boldsymbol{A}_p B_n$ in the local area of active region NOAA 9033 in 2000 June. White (black) contours mark positive (negative) rate of change G of magnetic helicity at ± 5, 20, 50, 100, 180 and 300 ($\times 10^{12}$ G^{2}m^{2}s^{-1}). The velocity arrows are inferred by the local correlation tracking technique. White (black) represents positive (negative) polarity of magnetic field.

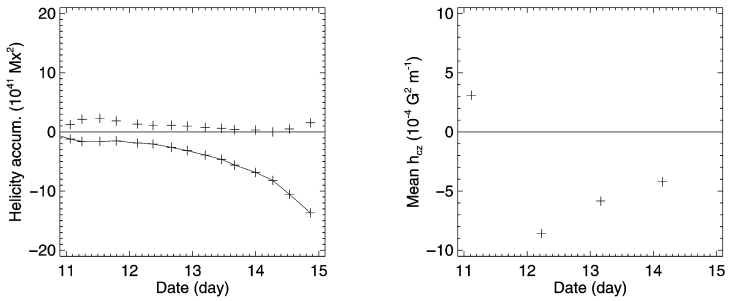

Fig. 7 Left panel shows the time profile of the accumulated change of magnetic helicity from the estimated dH/dt in the local area of active region NOAA 9033 shown in Fig. 6. Right panel shows the time profile of the total helicity in the active region.

X-ray configurations and the emission cores in the active region are shown in Figure 10. These provide the large-scale magnetic field in the high solar atmosphere. By comparing the evolution of the highly sheared vector magnetic field between the magnetic poles 'N1' and 'S1' in Figure 8 with the TRACE features in Figure 9 and soft X-ray configuration in Figures 9 and 10, we can infer a possible course of formation of the highly sheared magnetic field above the photosphere in the active region.

One believes that the soft X-ray loops at 01:53:04 UT on July 11 showed a potential-like field and connected the photospheric footpoints of opposite polarities (even if the projection effects are significant), while the post soft X-ray loop of the "Bastille Day" powerful flare at 17:09:21 UT on July 14 showed the relaxing of magnetic lines of force above the photosphere. It is noticed that an inverted "sigmoid" configuration was formed as the magnetic shear of the photospheric transverse field near the magnetic neutral line decreased on July 12–14 gradually before the flare. The inverted "sigmoid" configuration was found well developed at 00:40:47 UT on July 14. It provides evidence of intense non-potentiality and helicity of magnetic field above the photosphere (Rust & Kumar 1996; Pevtsov et al. 1997). The mean value of the force free field parameter α is about $2.0 \times 10^{-8}\mathrm{m}^{-1}$ in the corona (cf. Pevtsov et al. 1997). We can conclude that the evolution of photospheric vector magnetic field and the corresponding relationship with TRACE 171 Å and soft X-ray features in active region NOAA 9077 provide the information that highly sheared magnetic field is transferred from the lower solar atmosphere to the corona in the active region before the "Bastille Day" powerful flare (Yuchyshyn et al. 2001), i.e., the highly sheared flux emerges and then squeezes the pre-existed magnetic field to form the non-potential configuration of the magnetic field above the photosphere (Zhang 2002) and the injection of magnetic helicity from the subatmosphere also.

4.2.2 Twisted Motion of Sunspots

Because of the magnetic frozen-in state in the photosphere, the proper motion of sunspot features provides some information on the evolution of magnetic field and enables us normally to infer the evolution of the magnetic field. The relevant data in active region NOAA 9077 were analyzed by Liu & Zhang (2001). Figure 11 shows the horizontal velocity pattern of photospheric features in the main part of active region NOAA 9077 on 2000 July 12–15. The velocity vectors are inferred using the local correlation tracking techniques from the white light images observed by TRACE on July 12 at 03:22:21 and 04:03:39 UT , on July 13 02:34:25 and 03:35:33 UT, on July 14, 08:05:55 and 09:22:47 UT, and on July 15 at 05:42:31 and 06:20:46 UT. The data provide a different way of analyzing the morphological evolution of the active region. It is noticed that the magnetic pole 'N1' moved westward on July 12 and 13, which is consistent with what was discussed above. Meanwhile, sunspot 'A' moved at a speed of about 0.1 km s^{-1} relative to 'B' on July 13–14. In the sunspot 'A', the photospheric penumbral features twisted around the umbra counter-clockwise, especially on July 14, in directions almost perpendicular to the photospheric transverse magnetic field. The

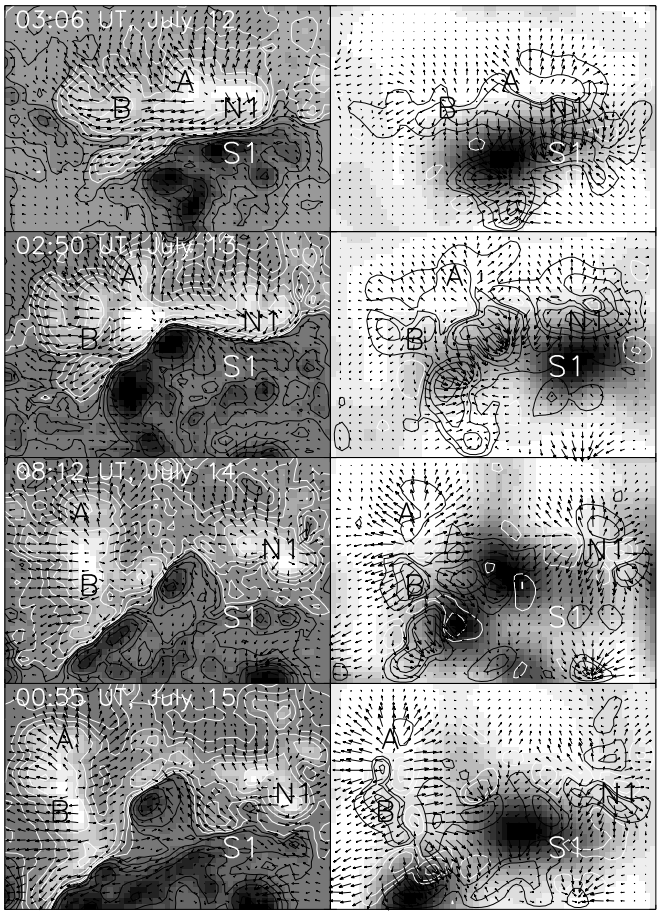

Fig. 8 Photospheric vector magnetograms in active region NOAA 9077 in July 2000 (left). The white (black) contours mark the positive (negative) polarity of ±50, 200, 500, 1000, 1800 and 3000 Gauss (left). The transverse magnetic field calculated in the approximation of magnetic charges in the solar surface (right). The dark areas mark high difference between observed and calculated transverse field, weighted by the observed field (right). The white (black) contours mark the photospheric current helicity density h_{cz} of ±5, 20, 100, 180 and 300 ($\times 10^{-3}\,\mathrm{G^2 m^{-1}}$) (right), which are inferred by the observational photospheric vector magnetograms. Size of the maps is $1.74' \times 1.21'$.

twisting speed near the outer edge of the sunspot 'A' is about $0.4\,\mathrm{km\ s^{-1}}$ on July 14. The speed is larger than the relative speed between the opposite magnetic poles 'N1' and 'S1'. Another similar instance of penumbral motion can be found in 'B' (see Figure 11), where the penumbral features also moved almost perpendicularly to the transverse field. It is largely consistent with the analysis of Brown et al. (2003). This means that if the rotation of sunspot features has been used to infer the twisted magnetic field or current (Leka et al. 1996), it will be slightly different from that calculated by the photospheric vector magnetograms (Wang et al. 1994).

The transverse field extends radially out from the umbrae and does not bring more information than is provided by the rotation of the sunspot features. Figure 8 shows that the difference (in direction) between the observed and calculated transverse field in the approximation of magnetic charges in the solar surface, weighted by the observed field, is not obvious in sunspot 'A', while it becomes significant near the highly sheared areas of the active region. Also, it can be found in Figure 9 that the extension of transverse field from the sunspots is almost consistent with

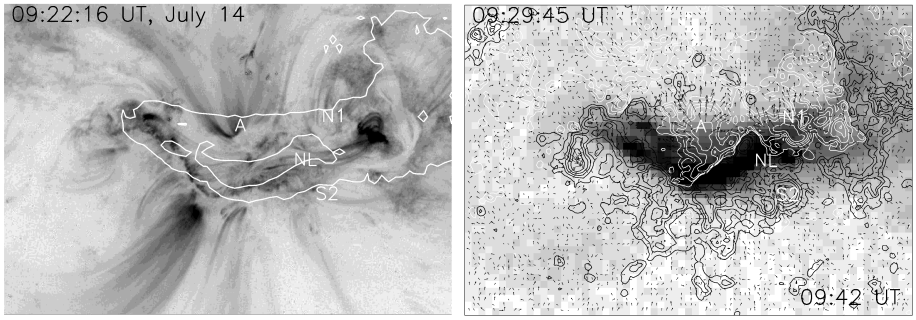

Fig. 9 TRACE 171 Å, soft X-ray and photospheric vector magnetic field in active region NOAA 9077 on 2000 July 14. The soft X-ray contours are drawn over the soft X-ray image in the left panel. The soft X-ray image is overlaid on the vector magnetic map in the right panel, where the solid (dash) contours mark positive (negative) polarity of ±50, 200, 500, 1000, 1800 and 3000 Gauss.

the orientation of TRACE 171 Å features, such as near 'A', 'N1' and 'S2'. This means that in complex active regions, photospheric mass does not strictly follow the magnetic lines of force. This is consistent with Figure 8 in places where the local current helicity density inferred from photospheric vector magnetograms does not show a tendency of increase with the rotation of sunspots. Comparing the basic geometric configuration of the spots, it is found that spot 'A' drew close to 'B' on July 12–14 due to the eastward motion of spot 'A'. This reveals that violent interaction and squeezing of different magnetic loops probably cause the twist motion of sunspot 'A'. By comparing the rotating direction of the magnetic poles with the magnetic shear in Figure 11, one can infer that the rotation of magnetic poles accompanies highly sheared emerging magnetic flux in the active region, i.e., the relative shear motion of photospheric footpoints of magnetic ropes 'N1' and 'S1' probably forces to take part the twist of other surrounding magnetic poles. We also notice that the interaction between the opposite poles 'N1' and 'S1' causes the shear of transverse field between them. The contribution in the rate of change of the magnetic helicity into the solar corona by the horizontal motion of the footpoints of the magnetic field in the solar surface on July 12–15 is shown in Figure 11. It shows that negative magnetic helicity is injected into the solar atmosphere near the magnetic pole 'N1' due to its shear motion on July 12–13, and near the magnetic pole 'A' due to its rotation on July 14, significantly.

The evolution of photospheric current helicity density h_{cz} in the active region NOAA 9077 is shown in Figure 8. Table 1 lists the numerical values of the photospheric mean current helicity density h_{cz} and of the rate of change of magnetic current helicity injected from the subatmosphere in Figures 8 and 11. It is noticed that the rate of change of magnetic helicity calculated from the white light images and photospheric vector magnetogram on July 15 is probably less accurate than the others, due to the larger difference in the time of observation of the magnetogram and the white light images on that day. Even then, the basic message on the injection of magnetic helicity is almost the same.

The accumulation of magnetic helicity above the photosphere inferred from the MDI longitudinal magnetograms by the local correlation tracking techniques over the whole of active region NOAA 9077 is shown in Figure 12. Significant injection of magnetic helicity and a decrease in the mean photospheric current helicity density before the "Bastille Day" flare have been found. It was demonstrated by Zhang (2002) that the high current helicity density in the photosphere was formed near the magnetic pole 'N1' in the vicinity of magnetic neutral line on July 12 and 13, and the "Bastille Day" flare on 2000 July 14 occurred after a decay of the current helicity density in the photosphere. It is consistent with the injection process of magnetic helicity discussed above, for the active region as a whole, even if the correlation between the change rate of magnetic helicity and photospheric current helicity density near magnetic structure 'A' (and 'B' also) on July 12–15

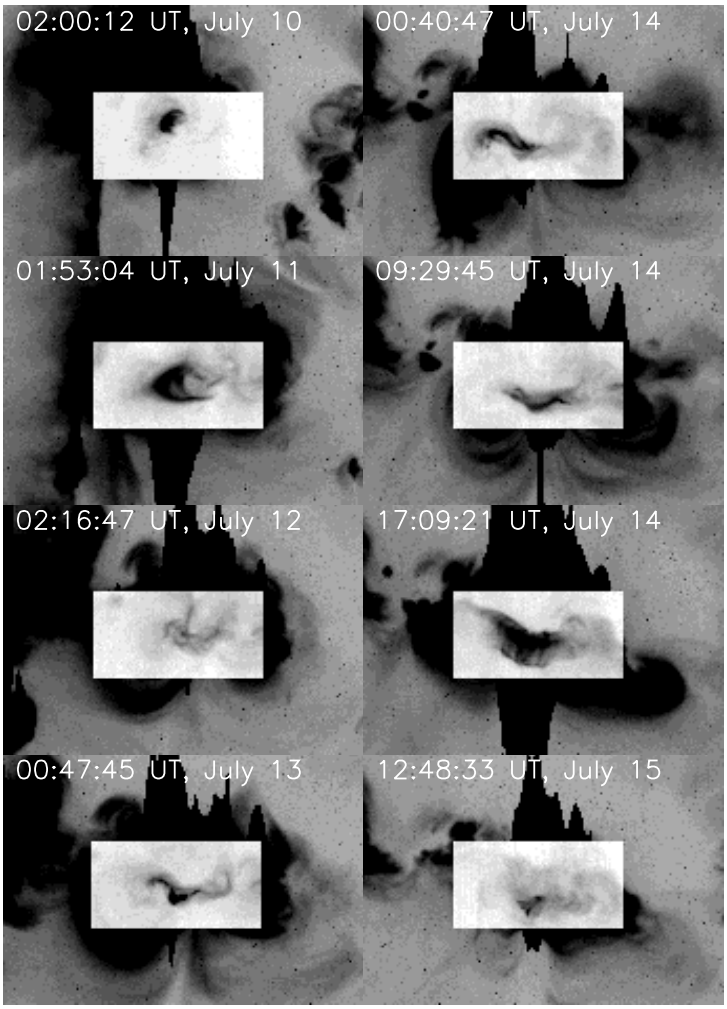

Fig. 10 A series of soft X-ray images of active region NOAA 9077 in 2000 July.

Table 1 Values of the injected rate of magnetic helicity and the corresponding mean current helicity density $\overline{hcz}$ in the main part of active region NOAA 9077 in Figures 8 and 11

Date	dH/dt $(10^{37}\mathrm{Mx}^2\ \mathrm{s}^{-1})$	$\overline{hcz}$ $(10^{-2}\mathrm{G}^2\ \mathrm{m}^{-1})$
July 12	–0.323	–3.51
July 13	–0.724	–5.73
July 14	–0.996	–1.53
July 15	–1.189	–0.46

is no more than a simple emerging flux region. This reflects the fact that the decrease of positive photospheric current helicity density is related to the injection of the magnetic helicity from the subatmosphere, as shown by the distribution of current helicity density near sunspot 'A' on July 13 and 14 in Figure 8.

In contrast to the twisting proper motion of penumbral features relative to the umbra, another line of evidence comes from observations of moving bipolar magnetic features and unipolar magnetic fragments from the main poles (Harvey & Harvey 1973; Zhang et al. 1992).

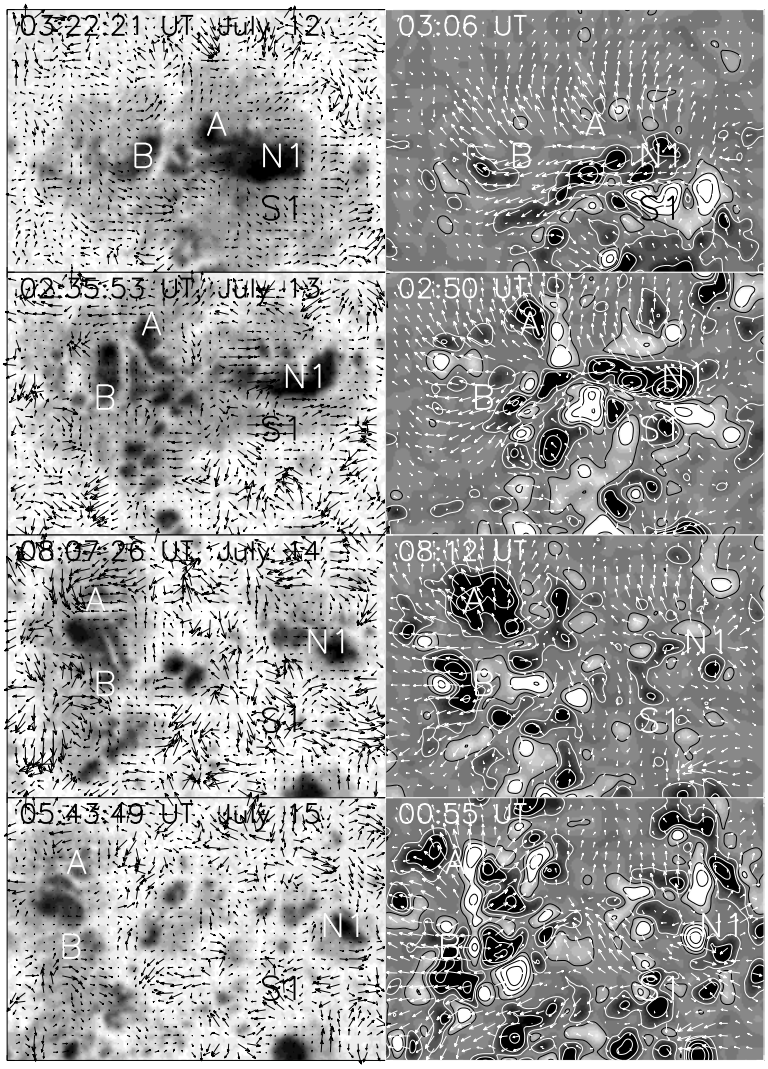

Fig. 11 Left: Horizontal velocity vectors (arrows) in active region NOAA 9077 in July 2000 overlaid on the white light image; Right: The contours represent $G = -2\boldsymbol{U}\cdot\boldsymbol{A}_p B_n$ inferred from the horizontal velocity vector and longitudinal magnetic field. The black (white) contours with white (black) areas mark the positive (negative) rate of change of magnetic helicity of ±5, 20, 50, 100, 180 and 300 ($\times 10^{13}\mathrm{G}^2\ \mathrm{m}^2\ \mathrm{s}^{-1}$). The arrows mark the transverse magnetic field.

This provides some basic information on the diffusion of magnetic features from the weighted center of the active region. It is found that the moving magnetic fragments (MMFs) at the outer edges of the sunspots moved almost along the direction of the photospheric transverse magnetic field and also is the orientation of the soft X-ray features. The mean speed of moving magnetic features is about 0.5–1.0 km s^{-1}, which is consistent with the previous results (Harvey & Harvey 1973). It is noticed that the the small-scale MMFs moved on the average faster than the large ones. They probably carry away magnetic energy from the the sunspots with their decay. Some of moving magnetic fragments of opposite polarities cancelled each other out near the magnetic neutral line. By comparing the moving twisted penumbral features and the MMFs, one can gain independent information on the motion of the sunspots. The rotation of sunspot magnetic field

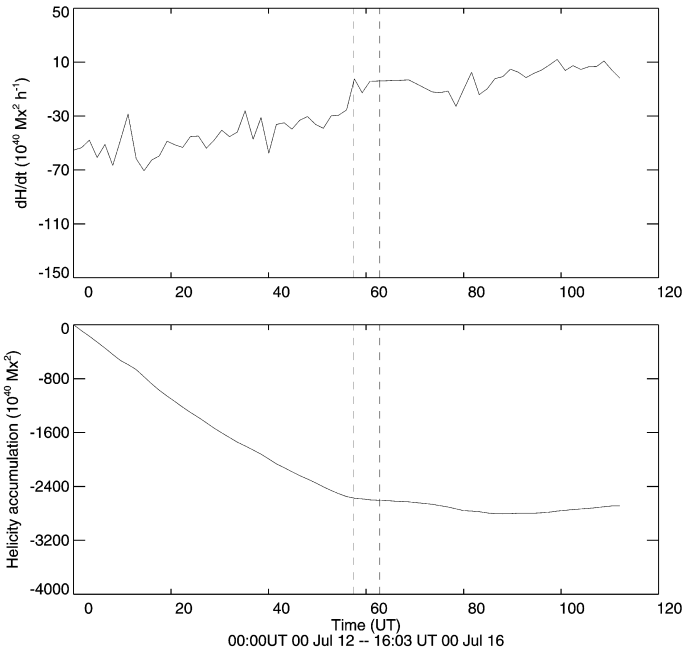

Fig. 12 Time profile of the accumulated change of magnetic helicity from the estimated dH/dt in active region NOAA 9077. The vertical dashed lines mark the begin and end times of the "Bastille Day" flare of 2000 July 14.

brings the magnetic (current) helicity into the higher solar atmosphere, but the MMFs probably reflect the breaking process of sunspot magnetic field and do not show a relation with the twisted motion of sunspots immediately: the MMF's form in the outer edges of sunspots, and reflect an independent motion relative to the rotating spot field.

5 SUMMARY

It has been shown that the horizontal motion of the footpoints of magnetic field in the photosphere probably not only provides the sliding of the magnetic field in the solar surface but also is the result of the emergence of magnetic flux from the subatmosphere, therefore, it also brings the magnetic helicity with emerging magnetic flux from the subatmosphere. The relationship between the magnetic and current helicity in the solar atmosphere should be found from a theoretical analysis of the solar atmosphere. Meanwhile, the calculation of the rate of change of magnetic helicity inferred from the horizontal velocity vector provides its transfer from the subatmosphere into the corona on the short time scale and on its accumulation. It involves different means of inferring the photospheric current helicity density from photospheric vector magnetograms observed at different times. As magnetic helicity is injected from the subatmosphere into the higher atmosphere, most of the magnetic helicity will probably not remain in the lower atmosphere. This results in differences in the detections between the injected rate of magnetic helicity above the photosphere and the photospheric current helicity density. In complex active regions, such as delta active regions, the relationship becomes more involved, because the injection of magnetic (current) helicity normally is connected not only with the emergence of magnetic field from the subatmosphere, but also with the violent interaction of different magnetic ropes.

We summarize the main results of this paper as follows:

(1) The magnetic and current helicity commonly provide some similar information on the handedness of twisted magnetic field. The injection of magnetic helicity from the subatmosphere and current helicity density in the photosphere contain some further information on the helical properties of the magnetic field. The former reflects the transfer process of magnetic helicity, while the later reflects the helical degree of magnetic field and relates only to the magnetic helicity remaining in the photosphere.
(2) It is found that the current helicity density in the photosphere evolves with the injection of magnetic helicity from the subatmosphere in flux emergence in active regions. The local sign change of the current helicity density in the photosphere is related to the injection of magnetic helicity of opposite sign. Moreover, some non-synchronism between them can be found also in their evolutions. As evidence from the delta active region NOAA 9077, the rotation of sunspots was found to be not in complete correspondence with the twist of the transverse field. It is known that the horizontal motion of magnetic field in the photosphere is probably related to the injection of magnetic helicity, while the change of vector magnetic field directly bears on the current helicity density.

Acknowledgements This study is supported by Grants 10233050, 10228307, 10311120115 and 10473016 of National Natural Science Foundation of China (NSFC), and TG 2000078401 of National Basic Research Program of China.

References

Abramenko V. I., Wang T. J., Yurchishin, V. B.:1996, Solar Phys., 168, 75
Ai G., Li W., Zhang H., 1982, Acta Astronomica Sinica, 23, 39
Ai G., Hu Y., 1987, Scien. Sinica A, 30, 868
Bao S. D., Zhang H. Q., 1998, AJ., 496, L43
Bao S. D., Zhang H. Q., Ai G. X. et al., 1999, ApJS, 139, 311
Bao S., Pevtsov A., Wang T. et al., 2000, Solar Phys., 195, 75
Berger M., Field G., 1984, J. Fluid Mech., 147, 133
Brown D., Nightingale R., Alexander D. et al., 2003, Solar Phys., 216, 79
Chae J., 2001, ApJ, 560, L295
Demoulin P. D., Berger M. A., 2003, Solar Phys., 215, 203
Harvey K., Harvey J., 1973, Solar Phys., 28, 61
Kleeorin N., Kuzanyan K., Moss D. et al., 2003, A&A, 409, 1097
Kusano K., Maeshiro T., Yokoyama T., Sakurai T., 2002, ApJ, 577, 501
Leka K. D., Canfield R. D., McClymont A. N. et al., 1996, ApJ, 462, 547
Longcope D., Fisher G., Pevtsov A., 1998, ApJ, 507, 417
Longcope D., Welsch B., 2000, ApJ, 545, 1089
Liu Y., Zhang H., 2001, A&A, 372, 1019
Nindos A., Zhang H., 2002, ApJ, 573, L133
Pevtsov A., Canfield R., Metcalf T., 1994, ApJ, 425, 117
Pevtsov A., Canfield R., Metcalf T., 1995, ApJ, 440, 109
Pevtsov A., Canfield R., McClymont A., 1997, ApJ, 481, 973
Rust D., Kumar A., 1996, ApJ, 464, L199
Seehafer N., 1990, Solar Phys., 125, 219
Wang J., 1996, Solar Phys., 163, 319
Wang H., Varaik J., Zirin H. et al., 1992, Solar Phys., 142, 11
Wang T., Xu A., Zhang H., 1994, Solar Phys., 155, 9
Yurchyshyn V. B., Wang H., Goode P. R. et al., 2001, ApJ, 563, 381
Zhang H., 2001a, MNRAS, 326, 57
Zhang H., 2001b, ApJ, 557, L71
Zhang H., 2002, MNRAS, 332, 500
Zhang H., Ai G., 1986, Acta Astronomica Sinica, 27, 226
Zhang H., Ai G., Wang H. et al., 1992, Solar Phys., 140, 307
Zhang H., Bao S., 1999, ApJ, 519, 876
Zhang H., LaBonte B., Li J. et al., 2003, Solar Phys., 213, 87